A Tri-Band Circular Microstrip Patch Antenna with Annular Slots for 5G Communications

Abdulguddoos S. A. Gaid [1], Osaid A. S. Qaid [2] and Mohamed H. M. Qasem[3]

[1,2,3] Dept. Of Communication and Computer Engineering
Faculty of Engineering, Taiz University, Yemen
[1] asry2000@hotmail.com
[2] osaid.ucv2016@gmail.com
[3] mohamedqasem270320@gmail.com

Abstract. This paper presents a multi-band circular microstrip patch antenna with annular slots and feeding line structure for 5G wireless devices and mm-wave applications. The proposed design is a tri-band resonating at 40.05GHz, 49.69GHz and 63.37GHz. To improve the antenna bandwidth and gain further, two annular slots are inserted to the circular radiating patch. The proposed structure is implemented on FR-4 epoxy dielectric substrate material with a relative permittivity (ε_r) = 4.4, a height (h) = 0.508 mm and a tangent loss (tanδ) = 0.02. A parametric analysis is carried out in order to achieve the optimum gain and bandwidth. The total radius of the optimized circular patch is 1.8 mm and the overall antenna size is 8× 7.6× 0.508 mm^3. The achievable fractional bandwidths are 6.64%, 20.4% and 11.72% of the tri-bands operating frequencies respectively. Moreover, simulated peak gains of 5.21 dBi, 5.23 dBi and 7.67 dBi are achieved at resonant frequencies 40.05/49.69/63.37GHz respectively. The proposed microstrip patch antenna was designed, simulated and optimized using the ANSYS High Frequency Structure Simulator software (HFSS). The proposed antenna is compact in size and provides wide impedance bandwidth and good gain.

Keywords: 5G Communications, Tri-band microstrip patch antenna, Circular patch Antenna, Annular slots.

1 Introduction

The wireless communication technology is one of the most growing technologies that has been widely used in modern communication systems. Especially interesting is the fifth generation (5G) wireless networks that are mainly designed to offer high data rates and to reduce the latency time by utilizing millimeter-waves spectrum and microstrip antenna technology. Due to these advantages, 5G wireless technologies including, Internet of Things (IoT), Device-to-Device (D2D) communication and smart cities represent the main direction in future wireless developments [1], [2]. There is a rapid increase demand for perfect antenna design to meet the great potential of millimeter-wave bands for 5G wireless applications and to overcome the problem of severe path losses associated with this part of spectrum. The required antennas should have high gains, wide bandwidths, and small size, lightweight, low-cost and low-power consumptions [3]. Microstrip antenna technology is appropriate candidate to achieve these requirements. However, the microstrip antennas are mostly omni-directional and inherently narrowband antennas where only up to 2% of band-width can be offered [4], [5], [6] and [7]. More importantly, in emerging 5G technologies, however, large bandwidths and high gains are necessary to trans-mit high data rates and to compensate for the inherited path loss in the millime-ter portion of electromagnetic spectrum [8], [9].

Numerous research papers have been published in the literature proposing tech-niques to enhance gain and bandwidth of the microstrip patch multiband anten-nas [10-17]. For instance, authors in [10] proposed a multiband microstrip an-tenna of 3×3 mm^2 patch dimensions on an RT/Duroid 5880. This patch is oper-ating at 30.9 GHz, 49.2GHz and 57.3GHz, with three impedance bandwidths of 2.2175 GHz, 3.4542 GHz and 3.1557 GHz at the resonant frequencies. Further-more, maximum gains obtained are 7.09 dBi, 7.6 dBi and 8.5 dBi at the center resonant frequencies.

Khattak et al [11] designed a dual- band elliptical microstrip patch antenna res-onates at 28/45 GHz with patch radius of 2 mm implemented on Rogers RT5880 with overall dimensions of 6 × 6 × 0.508 mm^3. Maximum gains of 7.6 dBi and 7.2 dBi with two impedance bandwidths 1.3 GHz & 1 GHz were achieved at the mentioned resonant frequencies. Furthermore, the maximum averaged gain is 7.4 dBi with a total bandwidth of 2.3 GHz over the two bands.

Imran et al [12] designed a dual-band antenna at 38/54 GHz integrated on Rog-ers RT5880 with substrate thickness of 0.508 mm, the patch size is 2×2 mm^2, achieving a maximum gain of 6.9 dBi & 7.4 dBi and bandwidths of 1.94 GHz and 2 GHz at the two resonant frequencies respectively. Moreover, a maximum averaged gain of 7.15 dBi and total bandwidth of 3.94 GHz are obtained over the two frequency bands.

A tri-band microstrip antenna operating at 50 GHz, 57 GHz and 63 GHz, with a patch size of 5×5 mm^2 implemented on 0.51 mm Rogers (RO3003) substrate thickness was proposed in [13]. The maximum gain averaged over the three bands is 5.66 dBi and impedance bandwidths of 1.2 GHz, 1GHz and 2 GHz are achieved.

Paper [14] proposed a dual-band microstrip antenna resonating at 28 GHz and 38 GHz, integrated on Rogers RT5880 with substrate thickness of 1.575 mm, the patch size is 20×20 mm^2, achieving impedance bandwidths (below -10dB return loss) of 4.7 GHz & 3.6 GHz and maximum gain of 5.75 dBi & 7.23 dBi were provided. Hence, a maximum averaged gain of 6.49 dBi and total band-width of 8.3 GHz are obtained over the frequency bands.

Additionally, a maximum gain of 3.3 dBi was obtained by the tri-band antenna designed in [15]. The antenna that operates at 28 GHz, 31.45 GHz and 34.6 GHz has a patch size of 4×3 mm^2, printed on RT5880 substrate with a thickness of 1.6 mm. The obtained bandwidth is 1.37 GHz, 0.11GHz and 2.4 GHz at the three bands respectively. Authors in [16] proposed a multiband antenna operat-ing at 10 GHz, 28 GHz and 38 GHz. This antenna has a size of 20×16.5×0.508

mm^3, printed on Rogers RT5880 substrate material. The maximum gain achieved is 5.67 dBi, 9.33 dBi and 9.57 dBi. Therefore, the maximum gain averaged over center frequencies is 8.19 dBi. In addition, the impedance bandwidths (<-10 dB return loss) of 0.343 GHz, 0.761 GHz and 1.5 GHz with a total of 2.604 GHz were obtained over the three bands. Moreover, a tri-band microstrip antenna operating at 24.4 GHz, 28 GHz and 38 GHz, was proposed by Kamal and Islam [17]. This antenna has a patch size of $3.4\times4.127\ mm^2$ printed on Rogers RT5880 with 0.25 mm substrate thickness. The maximum achievable gain is 6.65 dBi, 7.02 dBi and 5.05 dBi at the three resonant frequencies, whereas, the bandwidth provided by this antenna is 0.53 GHz, 0.9 GHz & 0.48 GHz at the three frequency bands respectively, with a total bandwidth of 1.91 GHz. Further, the maximum averaged gain achieved over the three resonant frequencies is 6.24 dBi.

In this paper, a tri-band circular microstrip patch antenna is proposed. The proposed antenna provides a wide impedance bandwidth over the three operating bands. The bandwidth and gain of the proposed antenna are improved by inserting two annular slots on the circular radiating patch. The proposed antenna can achieve a better bandwidth and a good gain in comparison with all the proposed antennas discussed above. However, the antenna is kept as small and low profile as possible. The impedance of the proposed structure is 20.32 GHz and the peak gain achieved is ranging from 5.21 dBi to 7.67 dBi.

This paper is organized as follows. The introduction and literature review are discussed in Section 1. Section 2 covers the design and optimization process through the parametric analysis. The simulation results are presented and discussed in Section 4. Finally, the conclusion is drawn in Section 5.

2 Antenna Design and Parametric Analysis

2.1 The Initial Antenna

The dielectric substrate selection is the first and most important step in the designing process of microstrip antennas. The antenna performance is highly influenced by the specifications of the substrate material like its height, dielectric constant and loss tangent ($\tan\delta$). The proper selection of the aforementioned parameters will result in a good design that achieves the desired performance.

There are many substrates that can be used for the design of microstrip antennas, and their dielectric constants are usually in the range of $2.2 \le \varepsilon_r \le 12$. The ones that are most attractive for good antenna performance are the thicker substrates whose dielectric constants are in the lower end of the range because they provide better efficiency, larger bandwidth, loosely bound fields for radiation into space, but at the expense of larger element size [18].

According to [19], the optimum performance will be obtained when the substrate thickness falls in the range,

$$0.003\lambda_0 \le h \le 0.05\lambda_0$$

where λ_0 is the resonant wavelength. In this paper, the low-cost RF-4 epoxy dielectric substrate material with a relative permittivity (ε_r) of 4.4, a height (h) of 0.508 mm and a tangent loss ($\tan\delta$) of 0.02 is selected. To get the resonance at 40 GHz, the initial dimensions of the circular patch are obtained by applying Equations (1) and (2). The actual radius (a) and the effective radius (a_e) of the circular patch are determined first and then optimized to get the optimum antenna characteristics [19].

$$a = \frac{F}{\left\{1+\frac{2h}{\pi\varepsilon_r F}\left[\ln\left(\frac{\pi F}{2h}\right)+1.7726\right]\right\}^{1/2}} \quad (1)$$

where $F = \frac{8.791\times10^9}{f_r\sqrt{\varepsilon_r}}$, h is the substrate thickness, f_r is the resonance frequency in hertz and ε_r is the dielectric constant of the substrate.

$$a_e = a\{1 + \frac{2h}{a\pi\varepsilon_r}\left[ln\left(\frac{\pi a}{2h}\right) + 1.7726\right]\}^{1/2} \quad (2)$$

The input impedance of the antenna should be matched with the source impedance, which equals to 50 Ω for all RF sources and microwave sources [20]. In this work, the inset-feeding technique is applied. After that, the antenna is optimized using HFSS simulator to get the optimum characteristics as required. A top view of the initial circular patch antenna is shown in Fig. 1.

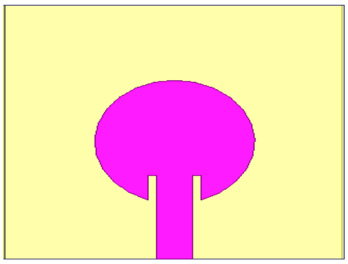

Fig. 1. The Initial Circular Patch Antenna Geometry.

2.2 The Final Optimized Design

The optimization process is performed using Ansys High Frequency Structure Simulator (HFSS) software. Two annular slots are etched on the circular patch to get the optimum characteristics in terms of return loss, gain and bandwidth. Fig. 2 and Fig. 3 show different views of the final optimized proposed design and Table 1 lists the optimized dimensions of the optimized proposed antenna.

The overall dimensions of the proposed antenna are $7.6 \times 8 \times 0.508$ mm^3 and the radius of the circular patch is 1.8 mm, with two etched annular slots on the circular radiating patch, which is printed on the top part of the substrate material. To improve the efficiency of the proposed antenna, a 50 Ω microstrip line through an inset feed is used to feed the radiating patch. In addition, a full metallic ground is located at the bottom of the dielectric substrate.

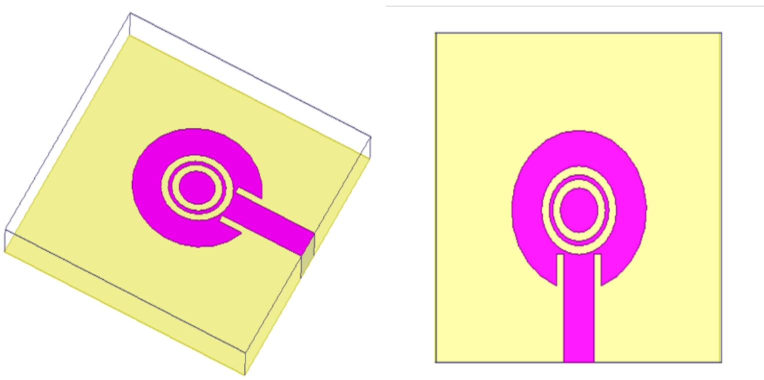

Fig. 2. The Optimized Antenna geometry a) The Perspective View b) The Top View.

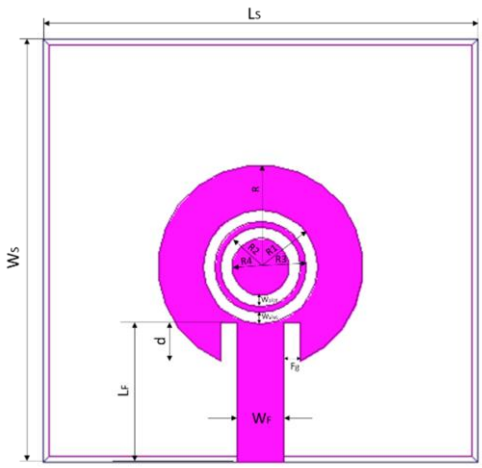

Fig. 3. The Proposed Antenna Geometry.

2.3 Parametric Analysis

The design of an efficient antenna requires a good understanding of how different parameters affect the antenna performance. The effect of varying antenna parameters including, the dimensions of the radiating patch, number, dimensions and shape of the etched slots and the inset distance of the microstrip feeding line are studied and simulated using HFSS simulator until we get the optimum design that fulfills all the specifications required.

Table 1. The Optimized Geometrical Dimensions of the proposed antenna.

Parameter	Symbol	Value (mm)
Patch Radius	R	1.8
Slot1 Outer Radius	R1	1
Slot1 Inner Radius	R2	0.8
Slot2 Outer Radius	R3	0.7
Slot2 Inner Radius	R4	0.5
Substrate Thickness	*h*	0.508
Substrate Width	W_S	8
Substrate Length	L_S	7.6
Inset Distance	F_i	0.82
Inset Gap	Fg	0.25
Feed Width	W_F	0.8
Feed Length	L_F	2.45

Etching slots on the radiating patch will produce a multiband characteristic and hence improve the bandwidth of the antenna [21]. Simulation shows that using more slots with changing the width of these slots enhances the return loss, produces wider bandwidth and higher gain. It could be seen from Fig. 4 and Table 2 that with two slots of 0.2 mm width, the total bandwidth of the three bands is equal to about 20.23GHz and the averaged gain over the three resonant frequencies is equal to 6.037 dBi, which are the best values we can get for this circular patch.

Fig.4 shows the return loss performance of the circular antenna with and without slots. When there are no slots on the radiating patch, there is only two resonant frequencies with a value of -16.15 dB at 39.64 GHz and -12.32 dB at 61.15 GHz and the total impedance bandwidth achieved is 5.422 GHz as can be seen from Table 2. Inserting annular slot into the radiating patch will improve the antenna's bandwidth by multi resonance characteristics. Another resonant frequency will appear and the patch will be a tri-band antenna. As a result, the return loss performance is substantially improved and hence the impedance bandwidth of the antenna becomes much wider. Table 2 reveals that by inserting a one annular slot, the S_{11} value is enhanced by a 64.3% at the first operating frequency, 195.2% at the second operating frequency and 52.6% at the third operating frequency. Further, the total impedance bandwidth is increased from 5.422 GHz to 17.333 GHz, which means an improvement of 219.7% is obtained. Inserting another annular slot will improve the impedance even further and the S_{11} values will be improved. Table 2 shows that the total impedance bandwidth is 20.23 GHz for the two slots case that is 273.1% improvement. Simulations show that the widest bandwidth is obtained with two annular slots with a width of 0.2 mm. Table 2 summarizes the values of S_{11}, gain and impedance bandwidth obtained for different number of annular slots.

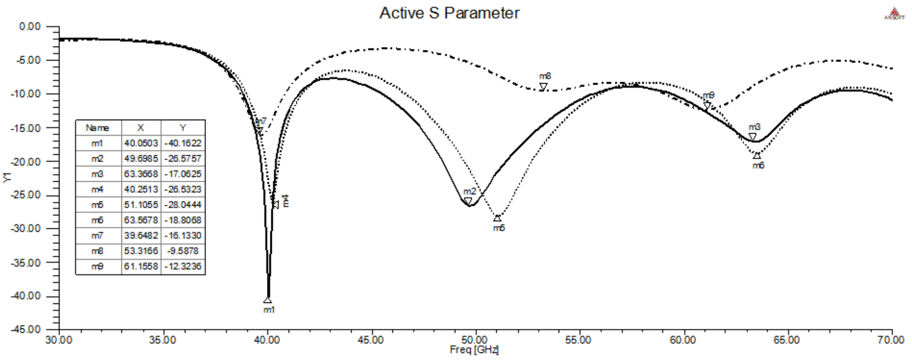

Fig. 4. Effect of varying number of slots on the simulated return loss (S_{11}) performance of the proposed antenna.

Table 2. Effect of varying number of slots on the performance of the proposed antenna.

# slots	Freq. (GHz)	S_{11} (dB)	Gain (dBi)	Avg. Gain (dBi)	BW (GHz)	Total BW (GHz)
Initial (no slots)	39.64	-16.15	5.43	6	1.946	5.422
	53.31	-9.5	6.77		-	
	61.15	-12.32	5.81		3.476	
1	40.25	-26.53	5.3	5.76	2.502	17.333
	51.1	-28.04	4.86		9.130	
	63.56	-18.8	7.12		5.701	
2	40.05	-40.16	5.21	6.037	2.66	20.23
	49.69	-26.57	5.23		10.14	
	63.36	-17.06	7.67		7.43	

Fig. 5 shows the simulated return loss performance versus frequency for different slot widths (W_{Slot}) and Table 3 summarizes the effects of different slot widths on the return loss, gain and impedance bandwidth of the proposed antenna. It is clearly seen that the highest gain is obtained for a slot width (W_{Slot}) of 0.25 mm, while at W_{slot} = 0.2 mm, the return loss values are the best and the impedance bandwidth achieved is the widest.

Fig. 6 and Table 4 show the return loss, gain and the bandwidth for different inset distances. The optimum gain and bandwidth are obtained for an inset distance (d) of 0.85 mm but the return loss values decrease as shown in Table 4.

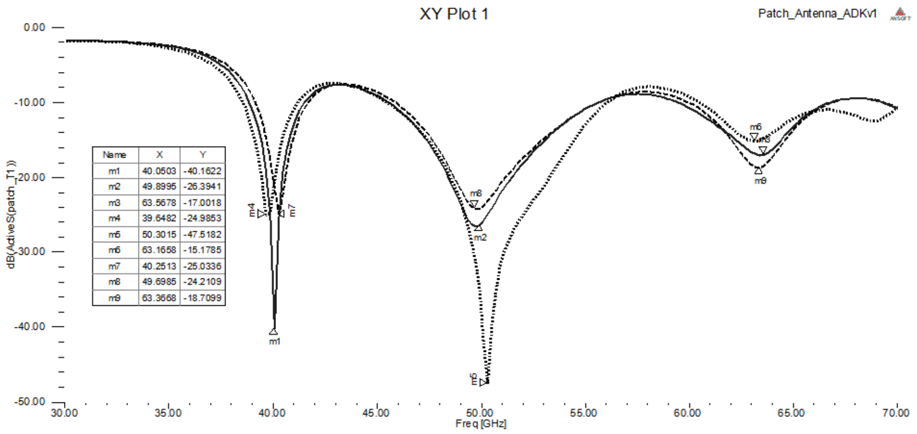

Fig. 5. Effect of varying slot's width (W_{Slot}**)** on the return loss performance of the proposed antenna.

W_{Slot} (mm	Freq. (GHz)	S_{11} (dB)	Gain (dBi)	Avg. Gain (dBi)	BW (GHz)	Total BW (GHz)
0.15	39.64	-24.98	5.234	5.827	2.66	19.13
	50.3	-47.51	5.37		10.6	
	63.16	-15.18	6.876		6.13	
0.2	40.05	-40.16	5.21	6.037	2.66	20.223
	49.69	-26.57	5.23		10.14	
	63.36	-17.06	7.67		7.43	
0.25	40.45	-26.45	5.4	6.118	2.55	19.3
	49.89	-19.32	5.23		9.82	
	64.17	-17.85	7.726		6.93	

Table 3. Effect of varying slot's width (W_{slots}) on characteristics of the proposed antenna.

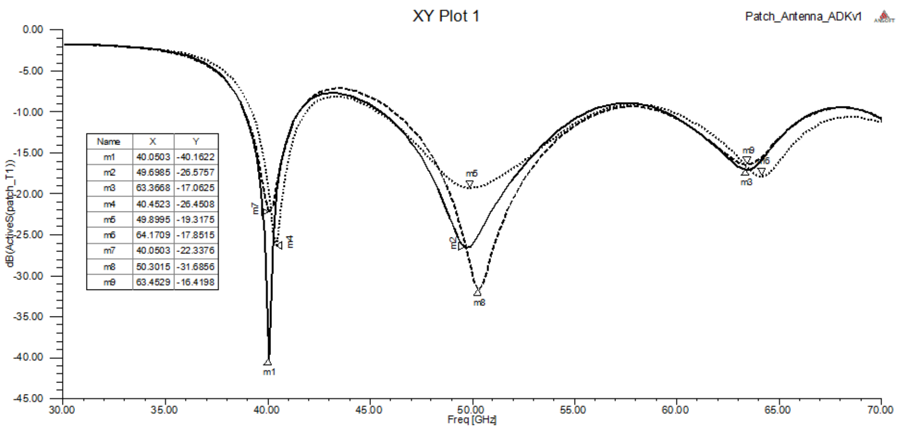

Fig. 6. Effect of varying inset distance (d) on the return loss performance of the proposed antenna**.**

Table 4. Effects of varying inset distance (d) on the proposed antenna performance.

Inset distance	Freq. (GHz)	S11 (dB)	Gain (dBi)	Avg. Gain (dBi)	BW (GHz)	Total BW (GHz)

(d) mm						
0.8	40.05 50.3 63.45	-22.34 -31.68 -16.42	5.29 5.09 7.75	6.043	2.68 10.22 6.583	20.546
0.82	40.05 49.69 63.36	-40.16 -26.57 -17.06	5.21 5.23 7.67	6.037	2.66 10.14 7.43	20.223
0.85	40.45 49.89 64.17	-26.45 -19.32 -17.85	5.26 5.25 7.76	6.09	2.666 10.75 8.6	22.02

Fig. 7 shows the return loss versus frequency for different feed widths (W_F). Table 5 outlines the effects of different feed widths on circular patch antenna performance. A maximum gain is obtained at a feed width (W_F) of 0.75 mm and higher bandwidth is achieved at a feed width (W_F) of 0.85mm. A tradeoff between the maximum gain and total bandwidth to enhance antenna performance is obtained at a feed width (W_F) of 0.8mm.

Fig. 8 and Table 6 describe the effect of inset gap (Fg) on antenna performance in terms of return loss, gain and bandwidth. A higher gain is obtained for inset gap (Fg) of 0.2 mm, while a wider bandwidth is achieved for inset gap (Fg) of 0.3 mm as shown in Table 6.

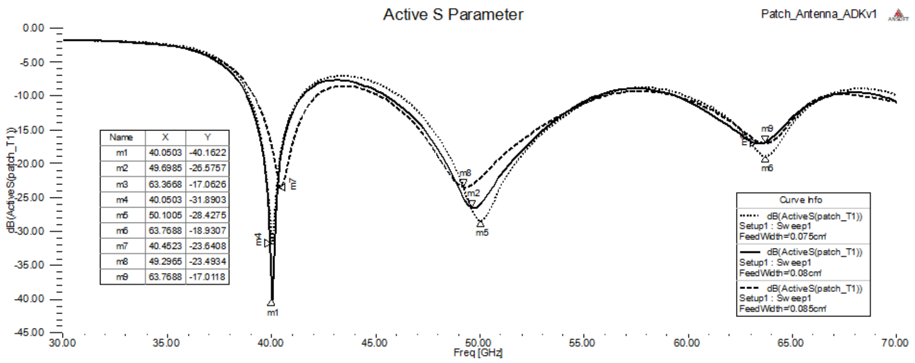

Fig. 7. Effect of varying feed width (W_F) on the proposed antenna return loss performance**.**

Table 5. Effect of varying different feed width (W_F) on the proposed antenna performance.

Feed Width (W_F) mm	Freq. (GHz)	S11 (dB)	Gain (dBi)	Avg. Gain (dBi)	BW (GHz)	Total BW (GHz)
0.75	40.05 50.1 63.77	-31.89 -28.43 -18.93	5.15 5.31 7.82	6.09	2.5 9.65 6.72	18.87

0.8	40.05 49.69 63.36	-40.16 -26.57 -17.06	5.21 5.23 7.67	6.037	2.66 10.14 7.43	20.223
0.85	40.45 49.3 63.77	-18.93 -23.49 -17.01	5.35 5.07 7.64	6.02	3 10.84 7.34	21.18

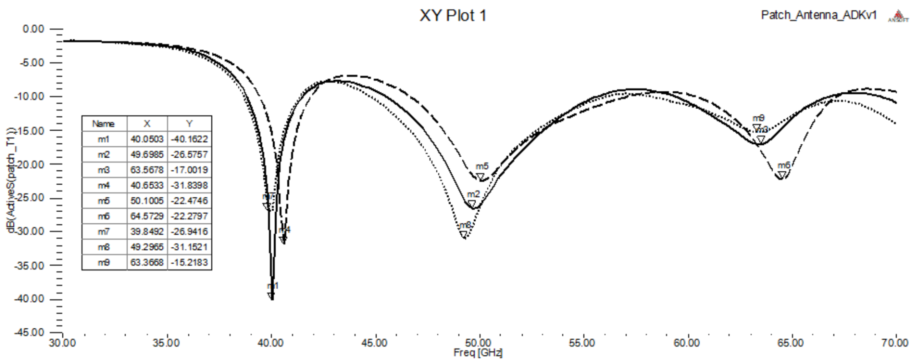

Fig. 8. Simulated S11 vs. Frequency for Different Inset Gaps (F_g).

Table 6. Effects of Different Inset Gaps on Circular Patch Antenna Performance.

Inset Gap (Fg) mm	Freq. Total (GHz) BW(GHz)	S11 (dB)	Gain (dBi)	Avg. Gain (dBi)	BW (GHz)
0.2	40.65	-31.84	5.12		2.44
	50.1	-22.47	5.23	6.06	10.45
	19.65				
	64.57	-22.28	7.83		6.76
0.25	40.05	-40.16	5.21		2.66
	49.69	-26.57	5.23	6.037	10.14
	20.223				
	63.36	-17.06	7.67		7.43
0.3	39.85	-26.94	5.34		2.69
	49.3	-31.15	5.13	6.027	
	11.055	22.555			
	63.36	-15.22	7.61		8.81

3 Simulation Results and Discussion

In this section, the simulation results of the proposed circular patch antenna are discussed. The simulated bandwidth and return loss versus frequency are illustrated in Fig. 9. The curve shows that peak return losses are 40.16 dB, 26.57dB and 17.06 dB at 40.05 GHz, 49.69 GHz and 63.36 GHz respectively. Moreover, impedance bandwidth of 2.66 GHz, 10.14 GHz and 7.43 GHz are achieved at the three operating bands. The total bandwidth over the three bands is about 20.223 GHz. The VSWR versus frequency is provided in Fig. 10. A VSWR of 1.02, 1.1 and 1.32 are obtained at 40.05 GHz, 49.69 GHz and 63.36 GHz respectively. the values of VSWR are in general less than 2 for all frequencies within the operating bandwidth of the optimized proposed antenna. The small values of the VSWR parameter reflect the good matching between the feeding line and the radiating circular patch, which in turn improves the radiation efficiency of the proposed antenna.

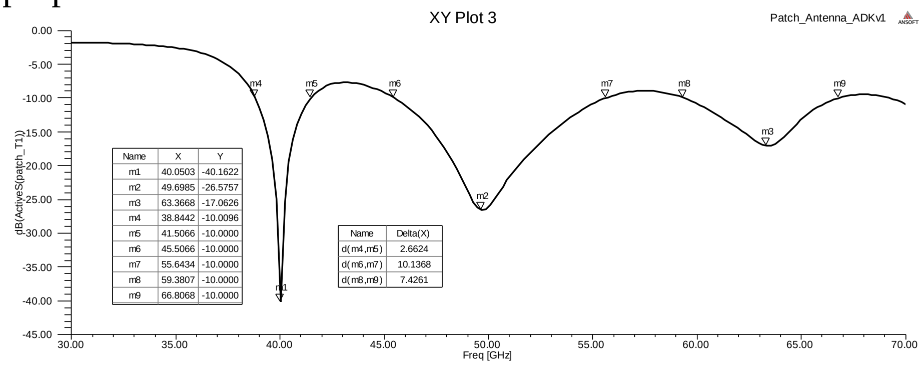

Fig. 9. The Simulated Return Loss vs. Frequency for the Optimized Antenna.

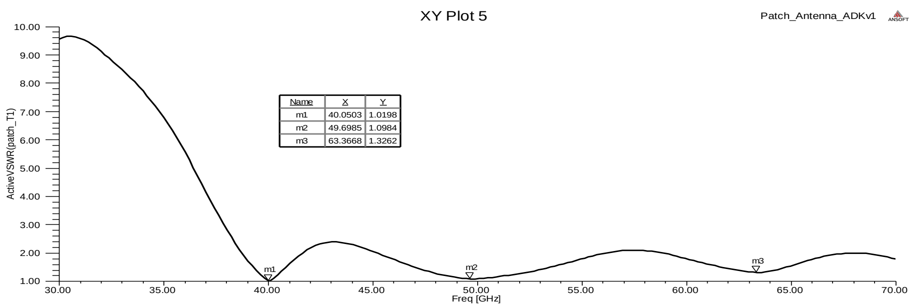

Fig. 10. The Simulated VSWR vs. Frequency.

Fig. 11 describes 3D radiation patterns of the proposed optimized antenna at the resonant frequencies. A maximum achievable gain of 5.21 dBi, 5.23 dBi and 7.67 dBi are achieved at the three operating frequencies respectively. The maximum gain averaged over the three center frequencies is 6.037 dBi. The gain could be further improved if this antenna design is extended to an array so that a gain that is required by the 5G applications is produced.

A comparison between the proposed antenna and some recent designs published in the literature is summarized in Table 7. The comparison is based on the patch size, the resonant frequencies, the return loss, the gain and the bandwidth. In terms of size, it is clearly seen that our design is smaller than other designs. Antennas presented in [11], [12], [14], [16] and [17] achieved better gain than the gain obtained by our proposed antenna, however the impedance bandwidths realized by these antennas are far below the impedance bandwidth achieved by the proposed antenna in this work as could be seen from Table 7. Our proposed design achieves an averaged gain of 6.037 dBi and an impedance bandwidth of 20.32 GHz.

Ref.	Patch Size(mm^2)	Freq. (GHz)	S11 (dB)	Gain (dBi)	Avg. Gain (dBi)	BW (GHz)	Total BW (GHz)
[10]	3×3	30.9 49.2 57.3	-36.5 -23.7 -14	2.23 3.45 3.16	2.95	7.09 7.6 8.5	8.83
[11]	Radius=2	28 45	-40 -14	7.6 7.21	7.405	1.3 1	2.3
[12]	2×2	38 54	-15.5 -12	6.9 7.4	7.15	1.94 2	3.94
[13]	5×5	50 57 63	-15 -22 -20	5.66	5.66	1.2 1 2	4.2
[14]	20×20	28 38	-40 -32.5	5.75 7.23	6.49	4.7 3.6	8.3
[15]	4x3	28 31.5 34.6	-12.5 -16.6 -15.7	3.3	3.3	1.37 0.11 2.4	3.88
[16]	……..	10 28 38	-25.8 -24.9 -32.9	5.67 9.33 9.57	8.19	0.343 0.761 1.5	2.64
[17]	3.4×4.127	24.4 28 38	-14.7 -19.3 -18.7	6.65 7.02 5.05	6.24	0.53 0.9 0.48	1.91
This Wor	Radius =1.8	40.05 49.69	-40.16 -26.57	5.21 5.23	6.037	2.66 10.14	20.3

k	63.36	-17.06	7.67	7.43

Table 7. A Comparative Analysis for Related Multiband Antenna Designs with This Work.

(a) (b)

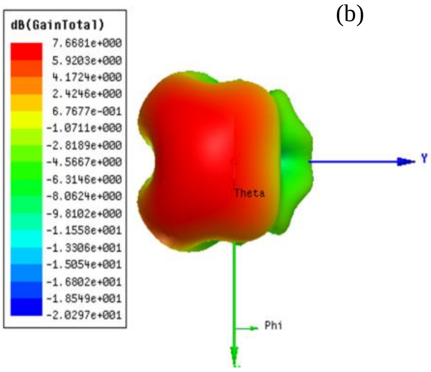

(c)

Fig. 11. The Simulated 3D gain at (a) 40.05 GHz (b) 49.69GHz (c) 63.36 GHz.

4 Conclusion

In this work, a compact, tri-band, circular patch antenna with two annular slots has been designed, optimized, and simulated using Ansys High Frequency
S o three bands and oper-
a achievable impedance
b 4 nd 7.43 GHz (11.72%)
r d is about 20.223 GHz
w d r frequencies is 6.037
d ons due to its compact
si

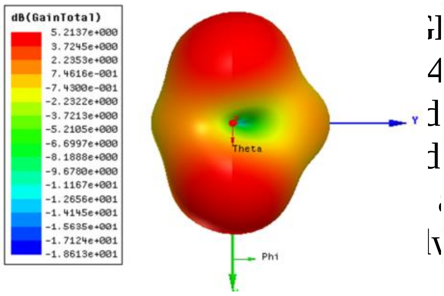

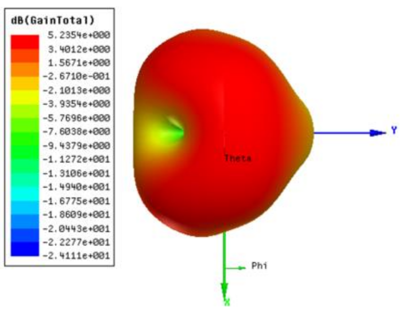

References

1. Kumar, S., Kaiwartya, O., Rathee, M., Kumar, N., Lloret, J.: Toward Energy-Oriented Optimization for Green Communication in Sensor Enabled IoT Environments. IEEE Systems Journal 99, 1-11 (2020).
2. Sabban, A.: Wideband Wearable Antennas for 5G, IoT, and Medical Applications. In Advanced Radio Frequency Antennas for Modern Communication and Medical Systems. IntechOpen. (2020)
3. El Gharbi, M., Fernández-García, R., Ahyoud, S., Gil, I.: A Review of Flexible Wearable Antenna Sensors: Design, Fabrication Methods, and Applications. Materials 13(17), 3781 (2020).
4. Gaid, A. S. A., Qaid, O. A. S., Ameer, M. A. A., Qaid, F. F. M., Ahmed, B. S. A.: Small and Bandwidth Efficient Multi-band Microstrip Patch Antennas for Future 5G Communications. In: Saeed, F., Mohammed, F., Gazem, N. (eds) IRICT 2019, Advances in Intelligent Systems and Computing, vol. 1073, pp. 653-662. Springer, Cham (2019).
5. Cao, W., Zhang, B., Liu, A., Yu, T., Geo, D., Wei, Y.: Gain enhancement for broadband periodic end fire antenna by using split-ring resonator structures. IEEE Transactions on Antennas and Propagation 60(7), 3513-3516 (2012).
6. Levine, E., Malamud, G., Shtrikman, S., Treves, D.: A study of microstrip array antennas with the feed network. IEEE Transactions on Antennas and Propagation 37(4), 426-434 (1989).
7. Mitha, T., Pour, M.: Conformal Wideband Microstrip Patch Antennas on Cylindrical Platforms. Progress In Electromagnetics Research 80, 1-6 (2018).
8. Mneesy, T. S., Hamad, R. K., Zaki, A. I., Ali, W. A.: A Novel High Gain Monopole Antenna Array for 60 GHz Millimeter-Wave Communications. Applied Sciences 10(13), 4546 (2020).
9. Anab, M., Khattak, M. I., Owais, S. M., Ali Khattak, A., Sultan, A.: Design and Analysis of Millimeter Wave Dielectric Resonator Antenna for 5G Wireless Communication Systems. Progress In Electromagnetics Research 98, 239-255 (2020).
10. Gaid, A. S., Qaid, O. A., Alhakimi, A. M.: Microstrip Antennas for Next Genertion Wireless Devices. In: First International Conference of Intelligent Computing and Engineering (ICOICE), pp. 1-4. IEEE, Hadhramout (2019).
11. Khattak, M. I., Sohail, A, Khan, U., Barki, Z., Witjaksono, G.: Elliptical slot circular patch antenna array with dual band behavior for future 5g mobile communication networks. Progress In Electromagnetics Research 89, 133-147 (2019).
12. Imran, D., Farooqi, M., Khattak, M., Ullah, Z., Khan, M., Khattak, M., and Dar, H.: Millimeter wave microstrip patch antenna for 5g mobile communication. In: International Conference on Engineering and Emerging Technologies (ICEET), pp. 1-6. IEEE, (2018).
13. Firdausi, A., Hakim, G., Alaydrus, M.: Designing a tri-band microstrip antenna for targetting 5g broadband communications. In: MATEC Web of Conferences, p. 03015. EDP Sciences, (2018).
14. Rahayu, Y., Hidayat, M. I.: Design of 28/38 GHz Dual-Band Triangular-Shaped Slot Microstrip Antenna Array for 5G Applications. In: 2nd International Conference on Telematics and Future Generation Networks (TAFGEN), pp. 93-97. IEEE, (2018).
15. Sumi, M., Hirasawa, K., Shi, S.: Two rectangular loops fed in series for broadband circular polarization and impedance matching. IEEE Transactions on Antennas and Propagation 52(2), 551-554 (2004).
16. Abdelaziz, A., Hamad, E. K.: Design of a compact high gain microstrip patch antenna for tri-band 5 G wireless communication. *Frequenz 73*(1-2), 45-52 (2019).

17. Kamal, M. S., Islam, M. J., Uddin, M. J., Imran, A. Z. M.: Design of a tri-band microstrip patch antenna for 5G application. In: *International Conference on Computer, Communication, Chemical, Material and Electronic Engineering (IC4ME2),* (pp. 1-3). IEEE, (2018).
18. POZAR, D. M.: Microwave engineering. New York. John Wiley & Sons. (2012).
19. Balanis, C.A.: Antenna theory: analysis and design. 4^{th} edn. John wiley & sons (2016).
20. Chakravarthy, S. S., Sarveshwaran, N., Sriharini, S., Shanmugapriya, M.: Comparative study on different feeding techniques of rectangular patch antenna. In: Thirteenth International Conference on Wireless and Optical Communications Networks (WOCN), pp. 1-6. IEEE, (2016).
21. Rao, J. C., Rao, N. V., Madhav, B. T. P., Vasavi, V., Vyshnavi, K.,Yadav, G. S. K.: Compact UWB MIMO slot antenna with defected ground structure. ARPN J. of Engineer. and Applied Sciences 11(17), 10487-10495 (2016).